

Accurate *ab initio* potential energy curve of $X^2\Pi$ state and high-temperature $A^2\Delta - X^2\Pi$ fluorescence spectra for CH radical

Jing Guo, Bing Yan*, and De-Ling Zeng

Institute of Atomic and Molecular Physics, Jilin University, Changchun 130012, China

Received 11 June 2012; Accepted (in revised version) 12 August 2012
Published Online 28 March 2013

Abstract. In present study an accurate *ab initio* potential energy curve of $CH(X^2\Pi)$ has been determined at the complete basis set limit. The core-valence corrections and relativistic corrections including scalar relativity and spin-orbit coupling are determined. The vibrational and rotational levels are calculated based on fitted potential energy curve. Total 19 vibrational levels are found for ^{13}CH ground state, and comparing with available experimental data, the deviation is less than 15 cm^{-1} . The dissociation energy is calculated within 50 cm^{-1} of the experimental value 29358 cm^{-1} . The $A^2\Delta - X^2\Pi$ electric transition dipole moment function is calculated, and the high-temperature fluorescence spectra arising from $A^2\Delta - X^2\Pi$ transition are simulated.

PACS: 31.15.aj, 31.30.jc, 33.15.Mt, 33.70.Ca

Key words: potential energy curve, relativistic effect, high-temperature fluorescence spectrum, CH radical

1 Introduction

Early in 1919 the CH radical was firstly detected by spectra analysis [1], and it becomes the subject of numerous theoretical and experimental investigations[2 4] since that time for its widely presence in the sun, stellar atmospheres, comets, interstellar spaces, flames and explosions. As most-studied free radical, previous spectroscopic data of CH have been collected and compiled by Huber and Herzberg[5] and are available online in NIST databases[6]. The spectroscopic studies on CH radical in optical, infrared, far-infrared, and microwave regions have well characterized ground and some excited states below

*Corresponding author. *Email address:* yanbing@jlu.edu.cn (B. Yan)

8eV[4,6,8]. While for some perturbed states via predissociation or those with weak transitions intensity, the *ab initio* studies are need to explore the molecular spectroscopic constants of high vibrational levels and molecular properties, such as equilibrium geometry, dissociation energy, dipole moment *et al.* For $X^2\Pi$ state of CH and its isotopic systems, only low vibrational levels spectroscopic constants are available because of the limitations in measurements. The high vibrational and rotational levels of $A^2\Delta$ state, crossing with $B^2\Sigma^-$ state, are difficult to characterize via A-X transition spectral experiments.

The *ab initio* investigations for CH became lasting interests for theoretical workers since 1954 [9]. In the past several decades, the spectroscopic constants of $X^2\Pi$ state were calculated using different theoretical approach including Hatree-Fock(HF), couple cluster, and configuration interaction(CI) methods with different number of basis functions [10,11]. Previous *ab initio* results [2] for equilibrium bond distance r_e of CH($X^2\Pi$) ranges from 1.09Å to 1.204Å, the smallest deviation between theoretical value and 1.1196Å of experimental value [6] is less than 10^{-3} Å. The error for harmonic frequency ω_e is at least 10 cm^{-1} , and that for anharmonic error $\omega_e x_e$ is in the range of $2\text{--}20\text{ cm}^{-1}$ in previous *ab initio* investigations[2] except those in Dunning's benchmark calculation [11]. While few early theoretical studies considered the relativistic effects, core electrons correlation corrections, and the complete basis set(CBS) limit extrapolation for the potential energy curve(PEC). And to the best of our knowledge, no *ab initio* reports for the spectroscopic constants of total vibrational and rotational levels with high level of theory as current electronic structure theory can yield.

In present work, the PECs of $X^2\Pi$ state were calculated with valence-splitting basis sets and extrapolated to CBS limit. The scalar relativistic effect, that is the mass-velocity and Darwin terms, the spin-orbit coupling (SOC) splitting, and the core correction energies were then evaluated. The total vibrational and rotational spectrum of $X^2\Pi$ state were obtained and compared with available experiments. The $A^2\Delta$ - $X^2\Pi$ transition dipole moment functions were calculated for simulation of vibrational-resolved high-temperature $A^2\Delta$ - $X^2\Pi$ fluorescence spectra which are important to explore the dynamics processes in combustion and plasma.

2 Methods and computational details

The C_{2v} symmetry was used in calculations, and the molecular axis was located along z-axis, thus the $^2\Pi$ and $^2\Delta$ states are represented by $^2B_1 + ^2B_2$ and $^2A_1 + ^2A_2$, respectively. The zeroth-order reference energies were calculated using full valence complete active space self consistent field (CASSCF)[12] wavefunctions with all-electron correlation-consistent polarized valence X-zeta, aug-cc-pVXZ($X=Q(4),5,6$), basis sets [11]. The valence electrons correlation energies were evaluated using internal contraction multireference CI(ic-MRCI) with singly and doubly excitations scheme as implemented in the Molpro[12] package. The Davidson corrections followed MRCI calculations (MRCI+Q) were used for size consistency consideration. For the X-tuple zeta basis sets, the zeroth-order

reference energies E_0 and correlation energies E_{CORR} approach the CBS limits according

$$E_0(X) = E_0(CBS) + a_0 \exp(-\alpha X), \quad (1)$$

and

$$E_{CORR}(x) = E_{CORR}(CBS) + a_c X^{-3}, \quad (2)$$

where a_0 , α , and a_c are parameters need to be determined [13]. We used $X=Q, 5, 6$ for formula (1), and $X=Q, 5$ for formula (2) to extrapolate the CBS energies. The core correlation corrections were evaluated by extrapolated full electron correlated and frozen core MRCI+Q/aug-cc-pCVXZ($X=CBS$) level. The spin-orbit coupling correction was calculated by state interaction technique with all 12 states correlated to first 5 dissociation limits included at CASSCF/aug-cc-pCVQZ level. Additional $2\alpha_1$ orbitals representing $3s\sigma$ and $3p\sigma$ orbitals of carbon atom were included in active space for SOC calculations. All calculations were performed in the range of 0.03–3.00 nm with grid of 0.005 nm, the $R=0.6$ nm was regarded as infinite limits.

The vibrational and rotational levels were obtained by numerically solving one-dimensional radial Schrödinger equation based on extrapolated and corrected PEC. The transition moments were derived from SOC calculations at different separate nuclear distances.

3 Results and discussion

3.1 *ab initio* potential energy curve

The valence PEC calculations were performed firstly, in which only correlation energies for electrons in $n=2$ valence shells of C atom and 1s electron of H atom were included. The zeroth-order (CASSCF in present work) energies and the dynamical correlation energies approaching the CBS were extrapolated separately. The valence active space CASSCF(5,5) wavefunctions at 53 internuclear distances from 0.04 to 0.6 nm for aug-cc-pVXZ basis sets with $X=Q, 5, 6$ as well as CBS limits were used to construct zeroth-order PEC. The sextuple-zeta energies differ from those of CBS by less 1.2 millihartree at all internuclear distances. The CBS extrapolations of dynamical correlation energies were performed following MRCI+Q/aug-cc-pVXZ($X=4, 5$) calculations, in which only singly and doubly excitations were considered, and no higher excitations were included in CI wavefunctions. Thus the valence CBS PEC was obtained.

To evaluate the core electrons correlation energies, the zeroth-order CASSCF wavefunctions were determined with active space of (7, 6). Subsequently, MRCI+Q calculations with and without the 1s core electrons of carbon atom correlated were separately performed. The aug-cc-pCVXZ($X=3, 4, 5$) basis sets were used, which include additional tight Gaussian functions to describe the inner core electrons comparing to aug-cc-pVXZ basis sets used for valence CBS PEC. The extrapolation scheme used for valence CBS PEC was repeated, and the core correlation corrections at CBS were finally obtained. The core correlation energies at different distances relative that at $R=0.6$ nm, that is $E(R)-E(0.6\text{nm})$,

are shown in Fig. 1. The core correlation corrections are prominent at all bond distance, and raise the PEC for $R > 0.125$ nm while lower the PEC for $R < 0.125$; the equilibrium bond distance will shift toward small value when core correlation energies are include. It should be noted that the absolute value of core correlation energies tend to increase at small internuclear distance, which is due to the large mixing between core orbitals with the valence orbitals as nuclear repulsive interactions rapidly raise. The core correlation corrections will lead less than 100 cm^{-1} increase for the equilibrium dissociation energy D_e .

The scalar relativistic energies were calculated by one-electron Douglas-Kroll approach [14] including the transformation to third order (DK3) at CASSCF/aug-cc-pCVQZ level. The scalar relativistic contributions to the PEC were then obtained by the energy differences between the total energies with and without DK3 terms at all bond distances. The scalar relativistic contributions to the PEC shown in Figure 1 were calculated as $E(R) - E(0.60 \text{ nm})$. It is clearly seen that the scalar contributions in the Franck-Condon region are positive and less than 20 cm^{-1} relative to the dissociation limit, and obviously the corrections decrease the dissociation energy.

The $2^4\Sigma^+$, $2(\Sigma^+, \Pi, \Delta)$, $2(\Sigma^-, \Pi)$, $4^6\Sigma^-$, and $2^4(\Sigma^+, \Pi)$ states, which adiabatically correlate to the five lowest dissociation limits $C(3P) + H(2S)$, $C(1D) + H(2S)$, $C(1S) + H(2S)$, $C(5S^0) + H(2S)$, and $C(3P^0) + H(2S)$, respectively, were coupled in SOC calculations to evaluate the spin-orbit splitting of 2Π state. The calculated spin-orbit splitting function $A(R)$ at CASSCF/aug-cc-pCVQZ level is present in Fig. 1. The spin-orbit splitting value A at experimental bond distance $R = 1.1196 \text{ \AA}$ is fitted to be 26.85 cm^{-1} , which is slightly lower than NIST value of 27.95 cm^{-1} . The SOC gives a shift of -13.5 cm^{-1} for Λ -S state $X^2\Pi$ at experimental bond distance, while its correction for dissociation energy is as small as less than 1 cm^{-1} because the energy at dissociation limit is simultaneously lowered in almost the same magnitude. The dipole moment function for $A^2 - X^2\Pi$ transition was calculated at same level of theory and illustrated in Fig. 1 (top and right axis).

As discussed above, 4 sets of PECs with various corrections have been obtained as follows:

- (i) CBS: PEC obtained as the CBS limit of singly and doubly valence-shell-only excitation MRCI+Q.
- (ii) CBS+SR: PEC containing, in addition to CBS, scalar relativistic corrections.
- (iii) CBS+SR+SO: PEC containing, in addition to CBS, not only scalar relativistic but also SOC corrections.
- (iv) CBS+SR+SO+CV: PEC containing, in addition to CBS+SR+SO also the core-electron correlation contributions.

To examine the relativistic and corrections effects on the spectroscopic constants, the D_e , ω_e , $\omega_e x_e$, and B_e were fitted for the above 4 PECs and listed in Table 1 with experimental value for comparison. The CBS, CBS+SR, and CBS+SR+SO PECs all give good accor-

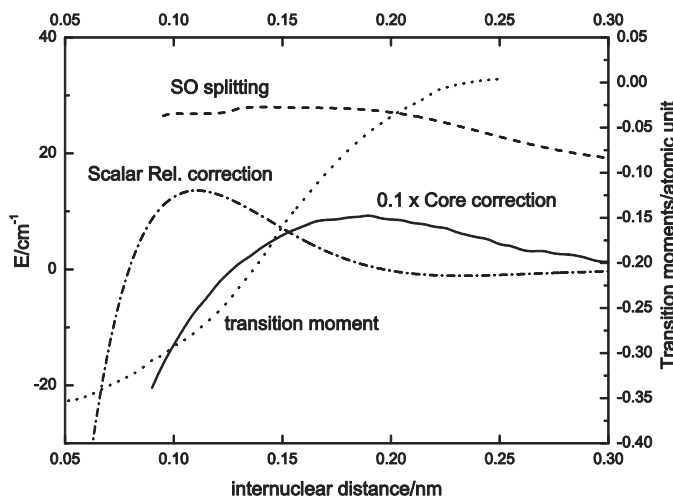


Figure 1: . Core correlation, Scalar relativistic corrections, and SO splitting at different internuclear distances (Left and Bottom); and the transition dipole moment function (Right and Top).

dance with experiment for the spectroscopic constants structural parameters. The deviations for bond distance is in the magnitude of 10^{-4}\AA , it is the most accurate theoretical estimate for equilibrium geometrical parameter of CH; The spectroscopic ω_e , $\omega_e x_e$, and B_e are almost the same as the experimental values, the relative errors are 0.002%, 0.5%, and 0.007%, respectively. For the dissociations energy, the values with relativistic corrections give a result of 29409 cm^{-1} with an improvement of 14 cm^{-1} . The core correlation corrections surprisingly do not lead the smallest errors of the spectroscopic parameters except for $\omega_e x_e$; the bond distance with additional core corrections is of $1.9 \times 10^{-3}\text{\AA}$ (0.09%) error, the errors for ω_e , $\omega_e x_e$, and B_e are 0.4%, 0.15%, and 0.35%, respectively; The dissociation energy is overestimated by 114 cm^{-1} with 0.4% error. One possible reason for the surprising deviation when induced core correction is the lack of higher excitation in valence orbitals considered in CBS procedure. The full CI calculation for CH ground state of course is not an expensive job, while it will be very difficult for other molecular systems with more electrons. One of the main goal is to examine the effects of various corrections to PEC, and according to current results CBS combined relativistic corrections (Scalar and SOC) approach is one of good approximations for PEC if no near-full CI efforts are made.

3.2 Rotation-vibration spectrum

The vibrational and rotational energy levels $E_{v,J}$, where v and J are vibrational and rotational quantum numbers, respectively, were obtained by numerically solved the radial equation,

$$-\frac{\hbar^2}{2\mu} \frac{d^2 \Psi_{v,J}(R)}{dR^2} + \left\{ \frac{\hbar^2}{2\mu R^2} [J(J+1) - \Omega^2] + V(R) \right\} \Psi_{v,J}(R) = E_{v,J} \Psi_{v,J}(R) \quad (3)$$

Table 1: The spectroscopic constants of CH.

	Experiment ^a	CBS	CBS+SR	CBS+SR+SO	CBS+SR+SO+CV
B_e	14.457	14.458	14.458	14.458	14.515
ω_e	2858.5	2859.61	2858.47	2858.47	2870.63
$\omega_e x_e$	63.0	62.73	62.71	62.71	63.09
D_e	29358.57	29422.63	29408.99	29408.98	29471.67
$R_e(\text{\AA})$	1.1199	1.1196	1.1196	1.1196	1.1180

^a NIST experimental values

in which μ is reduced mass of molecule, Ω is electronic angular momentum along molecular axis, and $V(R)$ is the potential energy function. Each energy level $E_{v,J}$ is the sum of vibrational term $G(v)$ and the sublevels of $F_v(J)$ which is represented by a power series expansion,

$$E_{v,J} = G(v) + B_v[J(J+1)] - D_v[J(J+1)]^2 + H_v[J(J+1)]^3 - L_v[J(J+1)]^4 + \dots \quad (4)$$

The CBS+SR PEC is used for effective $V(R)$ in equation (3), and total 19 vibrational levels are found for ^{13}CH ground state with present theoretical approach. The vibrational terms and centrifugal distortion constants (B_v , D_v , H_v , L_v) associated with the expansion are listed in Table 2. The experimental values of first 4 vibrational levels are collected for comparisons. The difference between present calculation and available experiment is in the range of $6\text{--}15\text{ cm}^{-1}$ with errors of 0.2%, and the error keeps unchanged for $v=1\text{--}3$.

For each vibrational level, the rotational constants were determined, as shown in third to sixth column in Table 2. The first 4 calculated B_v differ from the experimental values in 10^{-3} cm^{-1} , and the calculated B_v vary regularly with vibrational quantum v . At least two significant digits of calculated D_v and H_v agree with available experiment. For L_v , the calculated values of $v=0$ and 1 agree well with experiment, while for large v the L_v has obvious deviation. Some calculated H_v and L_v values with numerical errors are not reported in Table 2. Briefly, the Table 2 reveals excellent agreement between theory and experiments, especially for B_v and D_v .

3.3 High-temperature $A^2\Delta - X^2\Pi$ fluorescence spectrum

The CBS+SR PEC for $A^2\Delta$ state was constructed with the same procedures as described in Section 3.1, the relative energy and the rotational constants for each vibrational levels are presented in Table 3. The $A^2\Delta$ state potential well only contains 9 bound levels according present theory of level, and calculated relative energies T_v are less than 0.2% comparing with previous measurement. The rotational constants B_v and D_v are in good accordance with experiments.

The Franck-Condon(FC) factor $f_{v'v''}$ between upper levels v' and lower levels v'' in $A^2\Delta - X^2\Pi$ transition were calculated based on the fitted CBS+SR PEC. For lower v' levels, only one transition is dominant for each v' . The f_{00} , f_{11} , f_{22} , f_{33} , and f_{44} were calculated

Table 2: The vibrational terms values and rotational constants for ^{13}CH ground state (unit in cm^{-1}). The experimental values in italic are collected in Ref. [3].

v	$G(v)$	B_v	$-D_v \cdot 10^3$	$H_v \cdot 10^7$	$-L_v \cdot 10^{11}$
0	0.0	14.110	1.455	1.166	1.426
	0.0	14.108	1.444	1.146	1.426
1	2719.69	13.588	1.432	1.134	1.442
	2725.16	13.582	1.422	1.127	1.386
2	5314.96	5325.02	13.068	13.061	1.414
	1.400	1.044 1.073	0.812	1.397	
3	7785.74	7800.99	12.550	12.543	1.384
	1.379	1.048	1.028	2.766	1.446
4	10135.81	12.035	1.377	1.055	-
5	12363.87	11.523	1.359	0.885	-
6	14471.07	11.006	1.361	0.786	-
7	16454.57	10.480	1.357	0.692	-
8	18313.09	9.946	1.363	0.570	-
9	20044.33	9.394	1.398	0.356	-
10	21642.30	8.815	1.452	-	-
11	23098.68	8.191	1.531	-	-
12	24403.16	7.513	1.678	-	-
13	25539.27	6.736	1.911	-	-
14	26486.47	5.846	2.276	-	-
15	27217.83	4.728	3.273	-	-
16	27658.83	2.943	4.843	-	-
17	27856.53	2.116	3.308	-	-
18	27969.39	1.412	2.294	-	-

to be 0.9944, 0.9882, 0.9899, 0.9892, and 0.9510, respectively, which agree excellently with experiment-derived values[3] 0.9913, 0.9802, 0.9810, 0.9864, and 0.9675. For higher levels $v' > 4$, more than one transitions become important because of the anharmonic effects, for example, in $6-v''$ transitions, f_{66} , f_{67} , and f_{68} are 0.4066, 0.2106, and 0.1596, respectively.

The lifetime of $\text{A}^2\Delta(v' = 0)$ was estimated with the same method in our previous work [15] to be $0.524 \mu\text{s}$ from calculated transition dipole moment function (in Fig. 1), 0-0 transition FC factor, and experimental A-X(0-0) energy spacing [3] $\nu_{00} = 23173.84 \text{ cm}^{-1}$, the calculated lifetime is close to the measured value of $0.565 \pm 0.020 \mu\text{s}$ [16]. The high-temperature vibrational resolved A-X fluorescence spectra were simulated via transition intensity formula $I = (2/3)m^2 \cdot \Delta E \cdot P$, where m is vibrational-averaged transition moment, E is energy between transition vibrational levels, and P is Boltzmann factor. Since the dissociation energy of $\text{CH}(\text{A}^2\Delta)$ is 2.01 eV ($46.35 \text{ kcal} \cdot \text{mol}^{-1}$), the fluorescence spectra at temperature T up to 20000 K , $T = 1500 \text{ K}$, 5000 K , 10000 K , 15000 K , and 20000 K were simu-

lated, respectively, and illustrated in Fig. 2. In calculations, we assume that all particles populate in $v' = 0$ level at 0K, the total particles population was normalized to unit, the Gaussian lineshape was used and the full width at half maximum(FWHM) value was chose as 2nm. The 0-0, 1-1, and 2-2 transitions centered at 431.5, 431.6, and 433.0nm, respectively, compose the strongest band, other transition cannot be observed even at high temperature $T=1500\text{K}$ under above assumptions. As temperature increasing, the intensities of other transitions become stronger, at $T=5000\text{K}$ the 3-3 transition(436.1nm) and 4-4 transition(441.7nm) become observable, the relative intensity to the strongest band is 5% and 3%. At 10000K, the relative intensity of 3-3 and 4-4 becomes 18% and 8%, respectively; at highest $T=20000\text{K}$, the relative intensity is approximately one third of the strongest band. Obviously, the temperature changes the intensity distribution of spectra via Boltzmann Law, while the large(1.0) FC factor for 3-3 and 4-4 transitions is one of intrinsic factors for the satellite spectra.

Table 3: Relative energy and rotational constants of $^{13}\text{CH A}^2\Delta$ state in cm^{-1} . The experimental values in italic are collected in Ref.3.

v	T_v^a	B_v	$D_v \cdot 10^3$
0	23173.84 ^b	14.42	1.539
	23173.84	14.49	1.547
1	25890.87	13.76	1.580
	25906.46	13.83	1.584
2	28413.75	13.04	1.655
	28447.00	13.11	1.650
3	30721.59	12.23	1.790
	30775.34	12.32	1.797
4	32785.00	11.30	2.029
5	34562.18	10.16	2.472
6	35994.17	8.71	3.347
7	37005.25	6.74	5.126
8	37548.36	4.29	8.252

^a Energy relative to $X^2(v=0)$, $T_v - T_0$ is $G(v)$ for A^2 state as used in Table 1.

^b Experimental value Y_{00} in Ref. [3] is used here.

4 Summary

The singly and doubly multireference configuration interaction method was employed to study the CH radical with complete basis set. The core correlation, scalar relativistic effects, and spin-orbit coupling contributions to the ground state potential energy curve were examined. It is found that the complete basis set extrapolation plus relativistic

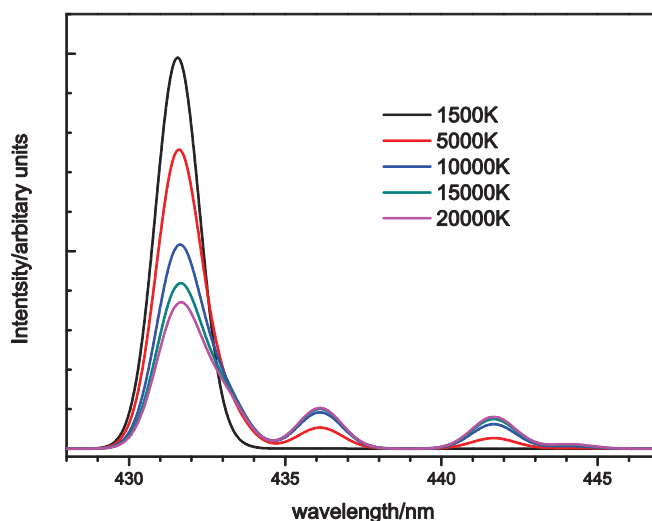


Figure 2: The high-temperature ${}^2\Delta - X^2\Pi$ fluorescence spectra of CH.

corrections is one of good approximations for potential energy curve if no efforts of full configuration interaction approach are made. The total 19 vibrational levels, rotational constants, and dissociation energy for ground state of CH are calculated and compared with experiments, excellent accordance between theory and experiments is found. The high-temperature $X^2\Delta - X^2\Pi$ fluorescence spectra ranged in 428 - 445nm were simulated, and found that the 0-0, 1-1, and 2-2 transitions are responsible for the band centered in 431.5nm, the two bands between 435nm and 445nm, arising from 3-3 and 4-4 transitions, could be observable at high temperature. The simulated spectra may be useful for high temperature spectral measurement and analysis.

Acknowledgments. This work is funded by National Magnetic Confinement Fusion Science Program of China under Grant No. 2010GB104003, the Fundamental Research Funds for the Central Universities under Grant No. 450060481375. We also acknowledge the High Performance Computing Center (HPCC) of Jilin University for supercomputer time.

References

- [1] T. Heurlinger and E Hulthen, Z. Wiss. Photogr. Photophys. Photochem. 18 (1919) 241.
- [2] A. Kalemios, A. Mavridis, and A Metropoulos, J. Chem. Phys. 111 (1999) 9536.
- [3] M. Zachwieja, J. Mol. Spectrosc. 182 (1997) 18.
- [4] G. Herzberg and J. W. C. Johns, Astrophys. J. 158 (1969) 399.
- [5] K. P. Huber and G. Herzberg, Molecular Spectra and Molecular Structure. IV. Constants of Diatomic Molecules (New York, Van Nostrand Reinhold, 1979), p.140.
- [6] NIST Chemistry Web Book, at <http://webbook.nist.gov/>

- [7] G. Herzberg and J. Shoosmith, *Nature* 183 (1959) 1801.
- [8] J. Higuchi, *J. Chem. Phys.* 22 (1954) 1339.
- [9] R. S. Grev and H. F. Schaefer III, *J. Chem. Phys.* 97 (1992) 8389.
- [10] K. A. Peterson, R. A. Kendall, and T. H. Dunning, *J. Chem. Phys.* 99 (1993) 1930.
- [11] H.-J. Werner, P. J. Knowles, R. Lindh, *et al.*, MOLPRO version 2006.1, a package of ab initio programs, see <http://www.molpro.net>
- [12] T. Helgaker, W. Klopper, and D. P. Tew, *Mol. Phys.* 106 (2008) 2107.
- [13] M. Douglas and N. M. Kroll, *Ann. Phys.* 82 (1974) 89.
- [14] B. Yan and W. Feng, *Chinese Phys. B* 19 (2010) 033303.
- [15] M. Ortiz and J. Campos, *Physica B* 114 (1982) 135.